ISSN 1674-1056
http://cpb.iphy.ac.cn
http://iopscience.iop.org/cpb
中国物理 B
Chinese Physics
中国物理 Chinese Physics B

# Entanglement teleportation via a couple of quantum channels in Ising-Heisenberg spin chain model of a heterotrimetallic Fe-Mn-Cu coordination polymer

Yi-Dan Zheng(郑一丹), Zhu Mao(毛竹), Bin Zhou(周斌)
**Citation:**Chin. Phys. B . 2019, 28(12): 120307 . **doi:** 10.1088/1674-1056/ab53cc
Journal homepage: http://cpb.iphy.ac.cn; http://iopscience.iop.org/cpb

**What follows is a list of articles you may be interested in**

---

## Plasmon mediated entanglement dynamics of distant quantum dots

Misbah Qurban, Rabia Tahira, Guo-Qin Ge(葛国勤), Manzoor Ikram
Chin. Phys. B . 2019, 28(3): 030304 . **doi:** 10.1088/1674-1056/28/3/030304

## The entanglement of deterministic aperiodic quantum walks

Ting-Ting Liu(刘婷婷), Ya-Yun Hu(胡亚运), Jing Zhao(赵静), Ming Zhong(钟鸣), Pei-Qing Tong(童培庆)
Chin. Phys. B . 2018, 27(12): 120305 . **doi:** 10.1088/1674-1056/27/12/120305

## Implementation of quantum phase gate between two atoms via Rydberg antiblockade and adiabatic passage

Xi Tan(谭曦), Jin-Lei Wu(吴金雷), Can Deng(邓灿), Wei-Jian Mao(毛伟建), Hai-Tao Wang(王海涛), Xin Ji(计新)
Chin. Phys. B . 2018, 27(10): 100307 . **doi:** 10.1088/1674-1056/27/10/100307

## Thermal quantum correlations of a spin-1/2 Ising-Heisenberg diamond chain with Dzyaloshinskii-Moriya interaction

Yidan Zheng(郑一丹), Zhu Mao(毛竹), Bin Zhou(周斌)
Chin. Phys. B . 2018, 27(9): 090306 . **doi:** 10.1088/1674-1056/27/9/090306

## Thermal entanglement of the spin-1 Ising–Heisenberg diamond chain with biquadratic interaction

Yi-Dan Zheng(郑一丹), Zhu Mao(毛竹), Bin Zhou(周斌)
Chin. Phys. B . 2017, 26(7): 070302 . **doi:** 10.1088/1674-1056/26/7/070302

---

# Entanglement teleportation via a couple of quantum channels in Ising–Heisenberg spin chain model of a heterotrimetallic Fe–Mn–Cu coordination polymer*

Yi-Dan Zheng(郑一丹), Zhu Mao(毛竹)†, and Bin Zhou(周斌)‡

*Department of Physics, Hubei University, Wuhan* 430062, *China*

(Received 11 July 2019; revised manuscript received 29 September 2019; published online 29 November 2019)

We investigate the teleportation of an entangled state via a couple of quantum channels, which are composed of a spin-1/2 Heisenberg dimer in two infinite Ising–Heisenberg chains. The heterotrimetallic coordination polymer $Cu^{II}Mn^{II}(L^1)][Fe^{III}(bpb)(CN)_2]\cdot ClO_4\cdot H_2O$ (abbreviated as Fe–Mn–Cu) can be regarded as an actual material for this chain. We apply the transfer-matrix approach to obtain the density operator for the Heisenberg dimer and use the standard teleportation protocol to derive the analytical expression of the density matrix of the output state and the average fidelity of the entanglement teleportation. We study the effects of the temperature $T$, anisotropy coupling parameter $\Delta$, Heisenberg coupling parameter $J_2$ and external magnetic field $h$ on the quantum channels. The results show that anisotropy coupling $\Delta$ and Heisenberg coupling $J_2$ can favor the generation of the output concurrence and expand the scope of the successful average fidelity.

**Keywords:** entanglement teleportation, Ising–Heisenberg chain, transfer-matrix approach, concurrence

**PACS:** 03.67.Bg, 03.67.Mn, 75.10.Pq **DOI:** 10.1088/1674-1056/ab53cc

## 1. Introduction

Quantum entanglement as an important physical resource has received much attention.[1] For an entangled system, there is the nonlocal correlation between its subsystems. It has been proved that the nonlocal correlation can be used to accomplish various quantum information processing tasks such as quantum teleportation,[2,3] quantum cryptographic key distribution,[4,5] quantum secret sharing,[6,7] and superdense coding.[8] Quantum teleportation was first proposed by Bennett *et al.* in 1993,[2] and they presented the standard teleportation protocol, in which a sender teleported an unknown quantum state to a distant receiver by sharing a pair of maximal entangled states with the receiver in advance. Since then, quantum teleportation has been extensively investigated both experimentally and theoretically.[3,9–15]

Earlier studies focused mainly on the teleportation of quantum states.[2,16–18] For contributing to entanglement manipulation, the entanglement teleportation gradually attracts researchers' attention. Lee and Kim investigated the entanglement teleportation of a two-body unknown entangled state via two identical kinds of noisy but independent quantum channels, and they found that the quantum channel must have the critical value of minimum entanglement in order to guarantee the entanglement teleportation of the initial state.[19] Due to the decoherence effect, the resource of maximally entangled state is hard to hold in real circumstance during teleportation. Thus, researchers pay more attention to the mixed entangled state as a resource. Popescu has shown that the mixed state as a quantum channel also has better fidelity than the classical one.[9] Furthermore, the standard teleportation protocol of an arbitrary mixed state as quantum channel has been proposed by Bowen and Bose in 2001.[10] Considering that the thermal fluctuation can destroy the quantum state, Arnesen *et al.* firstly investigated the thermal entanglement in a one-dimensional Heisenberg model.[20] Since then, a number of studies on the thermal entanglement have been conducted in various condensed matter systems.[21–24] Moreover, teleportation via the thermally entangled state has also attracted much attention.[25–33]

The Heisenberg spin chain as one of the simplest solid state systems has been studied extensively in the quantum teleportation, including the two-qubit $XX$,[25] $XY$,[26] $XXX$,[27] $XXZ$ Heisenberg models,[30] the three-qubit Heisenberg model with the Dzyaloshinsky–Moriya interaction,[32] and so on. In view of practical applications, it is necessary to study the model describing real materials. For example, $Cu_3(CO_3)_2(OH)_2$, known as natural azurite, can be described by the generalized diamond chain.[34] Rojas *et al.* used the standard teleporatation protocol to study an arbitrary entangled state teleportation through a couple of Heisenberg dimers in an infinite Ising–Heisenberg diamond chain.[33] Due to a high energy barrier for the spin relaxation, the single-chain magnets (SCMs) have been deemed to be a

*Project supported by the National Natural Science Foundation of China (Grant No. 11274102), the New Century Excellent Talents in University of Ministry of Education of China (Grant No. NCET-11-0960), and the Specialized Research Fund for the Doctoral Program of Higher Education of China (Grant No. 20134208110001).

†Corresponding author. E-mail: maozhu@hubu.edu.cn

‡Corresponding author. E-mail: binzhou@hubu.edu.cn

© 2019 Chinese Physical Society and IOP Publishing Ltd 

class of advanced materials which can be applied to quantum computing.[35–39] The Ising–Heisenberg diamond chain is one of representative of SCMs, and the magnetic frustration, the field induced phase transitions and the entanglement have been predicted in this heterometallic chains.[40–43] Moreover, it is suggested that heterotrimetallic complexes will have more intriguing magnetic properties than those in heterobimetallic complexes. Wang *et al.* used a stepwise method to synthesize the first heterotrimetallic coordination compounds $Cu^{II}Mn^{II}(L^1)][Fe^{III}(bpb)(CN)_2]\cdot ClO_4\cdot H_2O$, abbreviated as Fe–Mn–Cu.[44] Two different magnetic metal ions $Fe^{3+}$ and $Mn^{2+}$ regularly alternate along the main chain axis of the polymeric coordination compounds, and $Cu^{2+}$ ion is laterally attached to each $Mn^{2+}$ ion. Recently, Souza *et al.* introduced a simple exactly solvable model to characterize the most essential features of the heterotrimetallic coordination compounds Fe–Mn–Cu.[45] The exchange coupling between $Fe^{3+}$ and $Mn^{2+}$ ions is assumed to be Ising-like, while the exchange coupling between $Cu^{2+}$ and $Mn^{2+}$ ions is assumed to be an anisotropic $XXZ$ Heisenberg interaction. They have investigated the magnetization processes and the quantum entanglement in the model.[45]

Inspired by the work of Souza *et al.*,[45] we study the entangled state teleportation through a couple of quantum channels composed of the Heisenberg dimers in the Ising–Heisenberg chain of the heterotrimetallic coordination compounds Fe–Mn–Cu. The magnetic structure of the considered compound and the bipartite quantum coupling which serves as a quantum channel are shown in Fig. 1(a), and the schematic drawing of teleportation is shown in Fig. 1(b).

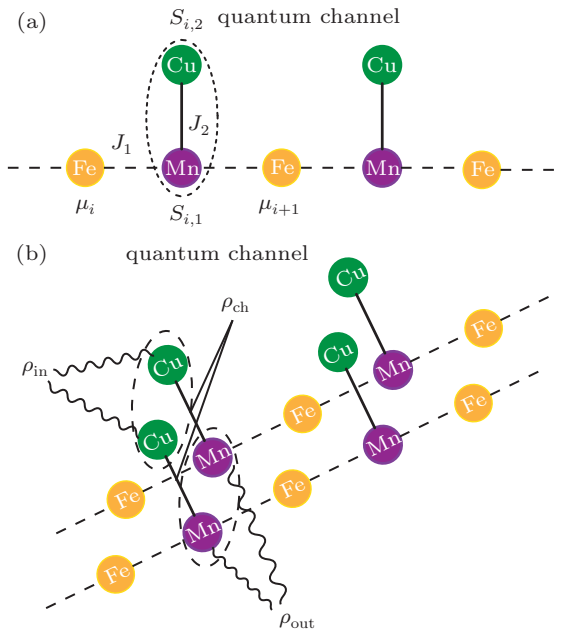



**Fig. 1.** (a) Magnetic structure of the Ising–Heisenberg spin chain of the heterotrimetallic coordination compounds Fe–Mn–Cu. The green, violet, and orange balls denote $Cu^{2+}$, $Mn^{2+}$, and $Fe^{3+}$ ions, respectively. The dashed lines indicate the Ising coupling, the solid lines represent the Heisenberg coupling, and the dashed box denotes the quantum channel. (b) A schematic drawing of the teleportation of the input state ($\rho_{in}$) via a couple of quantum channels ($\rho_{ch}$). The output state of teleportation is denoted as $\rho_{out}$.

The rest of the paper is organized as follows. In Section 2, we introduce the Hamiltonian of the infinite Ising–Heisenberg chain, and use the transfer-matrix approach to obtain the density operator of the quantum channel. Using the standard teleportation protocol, we obtain the density matrix expressions of the output state. We study the concurrence of the output state and the fidelity of the entanglement teleportation in Section 3. The conclusions will be presented in Section 4.

## 2. Model and methods

We consider the Heisenberg dimer of the Ising–Heisenberg spin chain of the heterotrimetallic coordination compounds Fe–Mn–Cu as the quantum channel (see the dashed box in Fig. 1(a)). The Hamiltonian of the Ising–Heisenberg spin chain can be expressed as follows:[45]

$$\mathscr{H} = \sum_{i=1}^{N} \mathscr{H}_i, \tag{1}$$

where

$$\begin{aligned}\mathscr{H}_i = & -J_1 S^z_{i,1}(\mu^z_i + \mu^z_{i+1}) - \frac{J_2\Delta}{2}(S^+_{i,1}S^-_{i,2} + S^-_{i,1}S^+_{i,2}) \\ & - J_2 S^z_{i,1}S^z_{i,2} - \frac{h_1}{2}(\mu^z_i + \mu^z_{i+1}) - h_2 S^z_{i,1} - h_3 S^z_{i,2}.\end{aligned} \tag{2}$$

Here $S_{i,1}$ represents the Heisenberg spin reflecting the $Mn^{2+}$ magnetic ion after renormalization of the respective magnetic moment, $S_{i,2}$ corresponds to the Heisenberg spin related to the $Cu^{2+}$ magnetic ion, $S^{\pm}_{i,j}$ denote the raising and lowering spin operators of spin-1/2, and $\mu^z_i = \pm 1/2$ stands for the Ising spin approximating the highly anisotropic $Fe^{3+}$ magnetic ion. $J_1$ and $J_2$ denote the Ising interaction between $Fe^{3+}$–$Mn^{2+}$ magnetic ions and the Heisenberg interaction between $Cu^{2+}$-$Mn^{2+}$ magnetic ions, respectively. $\Delta$ is the anisotropy parameter. Zeeman's terms ($h_1 = g_1\mu_0 h$, $h_2 = g_2\mu_0 h$, $h_3 = g_3\mu_0 h$) are involved in the Hamiltonian with $h$ being the external magnetic field, and we will consider the specific values ($g_1 = 2.4$, $g_2 = 10.0$, $g_3 = 2.2$) of the gyromagnetic factor according to the individual magnetic ions. Here $\mu_0$ is the Bohr magneton which will be set to unity ($\mu_0 = 1$) in the calculation. According to the experimental result, Souza *et al.* studied the quantum entanglement in this model for the antiferromagnetic coupling $J_2 < 0$.[45] In addition, the periodic boundary condition ($\mu_{N+1} = \mu_1$) is considered here for convenience.

Based on the expression of $\mathscr{H}_i$, it is easy to find $[\mathscr{H}_i, \mathscr{H}_j] = 0$. Thus we can adopt the transfer-matrix approach to gain the entanglement measurement of this infinite chain. The calculation process of the transfer-matrix approach has been presented detailedly in the literature.[40,42] Firstly, we obtain the eigenvalues of $\mathscr{H}_i$ by diagonalization of the two-qubit Heisenberg spin dimer and by assuming fixed values for $\mu_i$ and $\mu_{i+1}$ as follows:

$$E_1(\mu_i, \mu_{i+1}) = -\frac{J_2}{4} - \frac{1}{2}[(h_1 + J_1)(\mu_i + \mu_{i+1}) + h_2 + h_3],$$

$$E_2(\mu_i,\mu_{i+1}) = -\frac{J_2}{4} - \frac{1}{2}[(h_1 - J_1)(\mu_i+\mu_{i+1}) - h_2 - h_3],$$
$$E_3(\mu_i,\mu_{i+1}) = \frac{J_2}{4} - \frac{1}{2}[h_1(\mu_i+\mu_{i+1}) + \sqrt{(J_2\Delta)^2+a^2}],$$
$$E_4(\mu_i,\mu_{i+1}) = \frac{J_2}{4} - \frac{1}{2}[h_1(\mu_i+\mu_{i+1}) - \sqrt{(J_2\Delta)^2+a^2}], \quad (3)$$

where $a = h_2 - h_3 + J_1(\mu_i+\mu_{i+1})$. The corresponding eigenstates based on the standard basis $\{|00\rangle, |01\rangle, |10\rangle, |11\rangle\}$ are given by

$$\begin{aligned}
|\psi_1\rangle &= |00\rangle, \ |\psi_2\rangle = |11\rangle, \\
|\psi_3\rangle &= \frac{a+\sqrt{(J_2\Delta)^2+a^2}}{\sqrt{(J_2\Delta)^2+(a+\sqrt{(J_2\Delta)^2+a^2})^2}}|01\rangle \\
&\quad + \frac{J_2\Delta}{\sqrt{(J_2\Delta)^2+(a+\sqrt{(J_2\Delta)^2+a^2})^2}}|10\rangle, \\
|\psi_4\rangle &= \frac{-a+\sqrt{(J_2\Delta)^2+a^2}}{\sqrt{(J_2\Delta)^2+(-a+\sqrt{(J_2\Delta)^2+a^2})^2}}|01\rangle \\
&\quad + \frac{J_2\Delta}{\sqrt{(J_2\Delta)^2+(-a+\sqrt{(J_2\Delta)^2+a^2})^2}}|10\rangle. \quad (4)
\end{aligned}$$

Then, we obtain the two-qubit operator $\rho$ by fixing $\mu_i$ and $\mu_{i+1}$ as follows:

$$\rho(\mu_i,\mu_{i+1}) = \sum_{i=1}^{4} \mathrm{e}^{-\beta E_i(\mu_i,\mu_{i+1})}|\psi_i\rangle\langle\psi_i|. \quad (5)$$

The two-qubit operator in the natural basis becomes

$$\rho = \begin{bmatrix} \kappa_{1,1} & 0 & 0 & 0 \\ 0 & \kappa_{2,2} & \kappa_{2,3} & 0 \\ 0 & \kappa_{3,2} & \kappa_{3,3} & 0 \\ 0 & 0 & 0 & \kappa_{4,4} \end{bmatrix}. \quad (6)$$

The expressions of the elements of the two-qubit operator (6) are too complex, thus we do not present them here.

The element of the reduced density operator for the quantum channel can be expressed as

$$\begin{aligned}
\rho_{ch_{i,j}} &= \frac{1}{Z_N}\sum_{\{\mu\}} w(\mu_1,\mu_2)\cdots w(\mu_{r-1},\mu_r)\kappa_{i,j}(\mu_r,\mu_{r+1}) \\
&\quad \times w(\mu_{r+1},\mu_{r+2})\cdots w(\mu_N,\mu_1), \quad (7)
\end{aligned}$$

where $Z_N$ is the partition function, $w(\mu_i,\mu_{i+1})$ is the element of the transfer matrix, and $\kappa_{i,j}(\mu_i,\mu_{i+1})$ is the two-qubit operator about $\mu_i$ and $\mu_{i+1}$. Considering all $i$ and $j$, one can obtain the reduced density matrix of the quantum channel as follows:

$$\rho_{\mathrm{ch}} = \begin{bmatrix} \rho_{1,1} & 0 & 0 & 0 \\ 0 & \rho_{2,2} & \rho_{2,3} & 0 \\ 0 & \rho_{3,2} & \rho_{3,3} & 0 \\ 0 & 0 & 0 & \rho_{4,4} \end{bmatrix}. \quad (8)$$

Now we apply the standard teleportation protocol to study the quantum teleportation in the Ising–Heisenberg chain considered above. Supposing that these two quantum channels are far from each other, we can ignore any possible coupling between them. According to the work by Bowen and Bose,[10] the standard teleportation through the mixed states can be regarded as a general depolarizing channel. When a two-qubit state $\rho_{\mathrm{in}}$ is teleported via the thermal states of two independent Ising–Heisenberg chains, the output state $\rho_{\mathrm{out}}$ is given as[10,25]

$$\rho_{\mathrm{out}} = \sum_{i,j=0,x,y,z} p_{ij}(\sigma_i\otimes\sigma_j)\rho_{\mathrm{in}}(\sigma_i\otimes\sigma_j), \quad (9)$$

where

$$\begin{aligned}
&p_{ij} = p_i p_j = \mathrm{tr}[E^i\rho_{\mathrm{ch}}]\mathrm{tr}[E^j\rho_{\mathrm{ch}}], \\
&E^i = \{|\Psi^-\rangle\langle\Psi^-|, |\Phi^-\rangle\langle\Phi^-|, |\Phi^+\rangle\langle\Phi^+|, |\Psi^+\rangle\langle\Psi^+|\},
\end{aligned}$$

and $|\Psi^\pm\rangle$, $|\Phi^\pm\rangle$ are the Bell states. Here $\sigma_i$ $(i = 0,x,y,z)$ are the unit matrix and three components of the Pauli matrices.

We consider an initial state of two qubits expressed as

$$|\psi_{\mathrm{in}}\rangle = \cos(\theta/2)|00\rangle + \mathrm{e}^{\mathrm{i}\phi}\sin(\theta/2)|11\rangle, \quad (10)$$

where $\theta \in [0,\pi]$, $\phi \in [0,2\pi]$, $\theta$ and $\phi$ are the polar and phase parameters. Then the initial state will be obtained by $\rho_{\mathrm{in}} = |\psi_{\mathrm{in}}\rangle\langle\psi_{\mathrm{in}}|$. The input concurrence, as the measurement of entanglement, is

$$C_{\mathrm{in}} = 2|\mathrm{e}^{\mathrm{i}\phi}\sin(\theta/2)\cos(\theta/2)| = |\sin\theta|. \quad (11)$$

According to Eq. (9), we can obtain the output state $\rho_{\mathrm{out}}$, which is expressed as

$$\rho_{\mathrm{out}} = \begin{bmatrix} \alpha & 0 & 0 & \beta^* \\ 0 & \gamma & 0 & 0 \\ 0 & 0 & \gamma & 0 \\ \beta & 0 & 0 & \eta \end{bmatrix}, \quad (12)$$

where

$$\begin{aligned}
\alpha &= (\rho_{2,2}+\rho_{3,3})^2\cos^2\frac{\theta}{2} + (\rho_{1,1}+\rho_{4,4})^2\sin^2\frac{\theta}{2}, \\
\beta &= \frac{1}{2}\mathrm{e}^{\mathrm{i}\phi}(\rho_{2,3}+\rho_{3,2})^2\sin\theta, \\
\gamma &= (\rho_{2,2}+\rho_{3,3})(\rho_{1,1}+\rho_{4,4}), \\
\eta &= (\rho_{2,2}+\rho_{3,3})^2\sin^2\frac{\theta}{2} + (\rho_{1,1}+\rho_{4,4})^2\cos^2\frac{\theta}{2}. \quad (13)
\end{aligned}$$

Next, we use the concurrence to measure the entanglement of the output state. The definition of the concurrence has been proposed by Wootters *et al.*,[46,47] which is expressed in terms of a matrix $R$ as follows:

$$R = \rho_{\mathrm{out}}(\sigma_y\otimes\sigma_y)\rho^*_{\mathrm{out}}(\sigma_y\otimes\sigma_y). \quad (14)$$

Here $\rho^*_{\mathrm{out}}$ is the complex conjugate of the matrix $\rho_{\mathrm{out}}$, and $\sigma_y$ denotes the $y$ component of the Pauli operator. Then the concurrence of the output state can be gained in terms of the eigenvalues of the matrix $R$,

$$C_{\mathrm{out}} = \max\{\sqrt{e_1} - \sqrt{e_2} - \sqrt{e_3} - \sqrt{e_4}, 0\}, \quad (15)$$

where $e_i$ are the eigenvalues of the matrix $R$ (assuming $e_1 \geq e_2 \geq e_3 \geq e_4$).

When the input state is a pure state, the teleportation performance is usually measured by the fidelity defined as[48]

$$\begin{aligned} F(\theta,\phi) &= \langle\psi_{\rm in}|\rho_{\rm out}|\psi_{\rm in}\rangle \\ &= \frac{\sin^2\theta}{2}[(\rho_{2,3}+\rho_{3,2})^2+(\rho_{1,1}+\rho_{4,4})^2-(\rho_{2,2}+\rho_{3,3})^2] \\ &\quad +(\rho_{2,2}+\rho_{3,3})^2. \end{aligned} \tag{16}$$

Since the teleported state is an unknown pure state, the efficiency of the quantum communication is characterized by the average fidelity[49]

$$\begin{aligned} F_{\rm A} &= \frac{1}{4\pi}\int_0^{2\pi} {\rm d}\phi \int_0^{\pi} F(\theta,\phi)\sin\theta\,{\rm d}\theta \\ &= \frac{1}{3}[(\rho_{2,3}+\rho_{3,2})^2+(\rho_{1,1}+\rho_{4,4})^2-(\rho_{2,2}+\rho_{3,3})^2] \\ &\quad +(\rho_{2,2}+\rho_{3,3})^2. \end{aligned} \tag{17}$$

In the following section, we specifically analyze the entangled state teleportation via a couple of quantum channels composed of a spin-1/2 Ising–Heisenberg chain.

## 3. Results and discussions

### 3.1. Entangled state teleportation

Firstly, we study how the output concurrence $C_{\rm out}$ is affected by the input concurrence $C_{\rm in}$ and the temperature $T$. In Fig. 2(a), $C_{\rm out}$ is illustrated as a function of $T$ with various $C_{\rm in}$ in the absence of the external magnetic field ($h=0$). It is shown that $C_{\rm out}$ is nonmonotonic when the temperature increases. As the temperature increases from zero, the entanglement remains unchanged firstly, then increases to the maximum, and then gradually reduces to zero when the critical temperature is reached. Taking $C_{\rm in}=1$ (the black line in Fig. 2(a)), for instance, $C_{\rm out}=0.8$ when $T=0.001$, with increasing the temperature, the output entanglement $C_{\rm out}$ gets the maximum 0.8603 ($T=0.171$), and then it goes down to 0 ($T=0.851$). In addition, it is easy to obtain from Fig. 2(a) that $C_{\rm in}$ affects the range of $C_{\rm out}$. The larger the input concurrence $C_{\rm in}$ is, the larger the maximum value of $C_{\rm out}$ is, and the higher the critical temperature $T$ is. It is noted that $C_{\rm out}$ is never as large as $C_{\rm in}$ in Fig. 2(a). This means that the entanglement of the initial state is lossy when passing through the quantum channel. In Fig. 2(b), we consider the case with the external magnetic field $h=0.1$. The variation trend of the curves in Fig. 2(b) is similar to that in Fig. 2(a). However, it is worth noting that the external magnetic field $h$ will suppress the generation of the output concurrence.

In Fig. 3, we investigate the effect of the anisotropy $\Delta$ of the quantum channel on the output concurrence $C_{\rm out}$. $C_{\rm out}$ as a function of $C_{\rm in}$ is plotted in Fig. 3(a) for $T=0.1$, $J_1=J_2=-1$, and the different anisotropy parameters $\Delta$. It is shown that, in the same case of anisotropy, the relationship between $C_{\rm out}$ and $C_{\rm in}$ is linear, the larger the input concurrence is, the larger the output concurrence is. Moreover, we can obtain the fitting equation of each line in Fig. 3(a) as follows:

$$\begin{aligned} C_{\rm out} &= -0.00659+0.219C_{\rm in} \quad (\Delta=0.5), \\ C_{\rm out} &= -0.00147+0.547C_{\rm in} \quad (\Delta=1), \end{aligned}$$

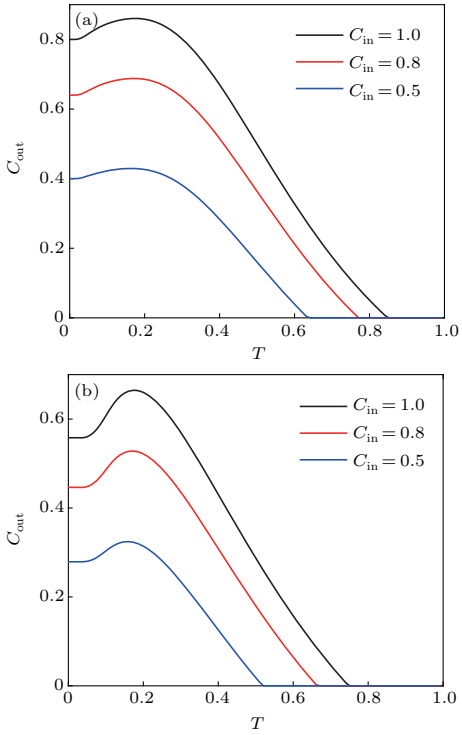



**Fig. 2.** Output concurrence $C_{\rm out}$ as a function of $T$ for $\Delta=2$, $J_1=J_2=-1$ with different values of $C_{\rm in}$: (a) $h=0$, (b) $h=0.1$.

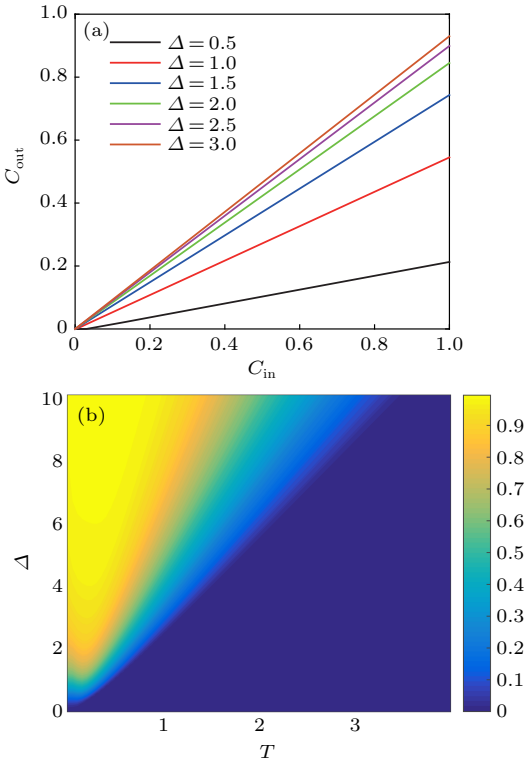



**Fig. 3.** (a) Output concurrence $C_{\rm out}$ as a function of $C_{\rm in}$ for $T=0.1$, $J_1=J_2=-1$, and different values of $\Delta$. (b) The density plot of the output concurrence $C_{\rm out}$ depending on the anisotropy parameter $\Delta$ and the temperature $T$ for $J_1=J_2=-1$ and $C_{\rm in}=1$. Here the external magnetic field is absented.

$$
\begin{aligned}
C_{\text{out}} &= -0.00019 + 0.743 C_{\text{in}} \quad (\Delta = 1.5),\\
C_{\text{out}} &= -0.00002 + 0.845 C_{\text{in}} \quad (\Delta = 2),\\
C_{\text{out}} &= 0.899 C_{\text{in}} \quad (\Delta = 2.5),\\
C_{\text{out}} &= 0.93 C_{\text{in}} \quad (\Delta = 3).
\end{aligned} \tag{18}
$$

From Eq. (18), it is shown that the slope of the line becomes larger and larger, finally approaches 1 with the increase of the anisotropy. The density plot of the output concurrence depending on $\Delta$ and $T$ for $C_{\text{in}} = 1$ is shown in Fig. 3(b). It also reveals that, in a certain range of anisotropy, with the increase of temperature, the tendency of the entanglement is to be promoted first and then suppressed. However, when the anisotropy exceeds this range, the temperature only inhibits entanglement. From Fig. 3, we can reach the conclusion that the stronger the anisotropy of the Heisenberg dimer as a quantum channel is, the higher the entanglement of the output state is.

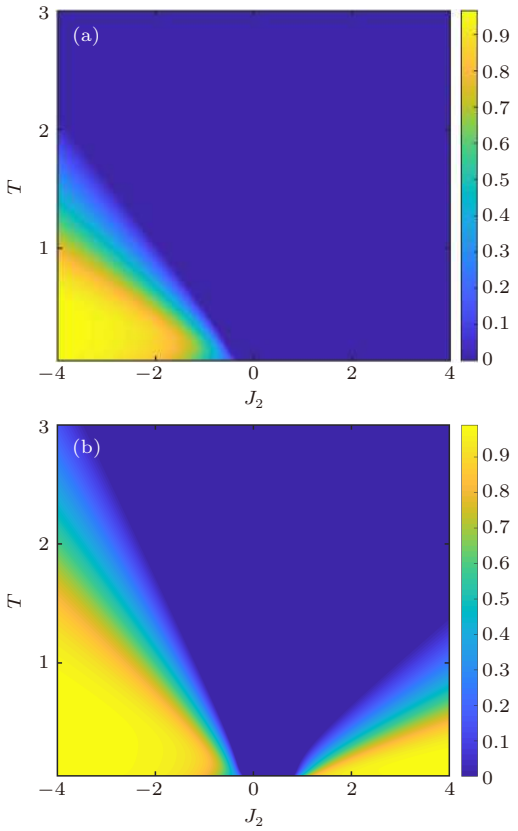



**Fig. 4.** Output concurrence $C_{\text{out}}$ as functions of $T$ and $J_2$ for $C_{\text{in}} = 1$, $J_1 = -1$ and $h = 0$: (a) $\Delta = 1$, (b) $\Delta = 2$.

In Fig. 4, we plot the output concurrence $C_{\text{out}}$ as a function of the temperature $T$ and the Heisenberg coupling parameter $J_2$ for $C_{in} = 1$, $J_1 = -1$, and $h = 0$. First, we study the case of isotropy $\Delta = 1$ in Fig. 4(a). It is shown that the output concurrence $C_{\text{out}}$ occurs only in the region of the antiferromagnetic coupling ($J_2 < 0$). There is no entanglement in the ferromagnetic region ($J_2 > 0$). For the ferromagnetic case ($J_2 < 0$), when $|J_2|$ is a small value, it is found that the output concurrence $C_{\text{out}}$ decreases with the temperature $T$ increasing. Taking $J_2 = -0.5$ as an example, $C_{\text{out}} = 0.20$ when $T = 0.01$, $C_{\text{out}}$ vanishes when $T$ is beyond 0.16. While $|J_2|$ is taken as a larger value, $C_{\text{out}}$ varies nonmonotonically with the temperature increasing. Taking $J_2 = -2$ as an example, $C_{\text{out}} = 0.80$ when $T = 0.01$. With increasing the temperature, the output entanglement $C_{\text{out}}$ reaches the maximum 0.87 ($T = 0.23$), and then it goes down to 0 ($T = 1.05$). Moreover, with the increasing $|J_2|$, the critical temperature corresponding to the vanishing of $C_{\text{out}}$ increases. For example, when $J_2 = -1$, $-2$, $-3$, and $-4$, the critical temperature $T_{\text{c}} = 0.49$, 1.05, 1.60, and 2.13, respectively. Figure 4(b) shows the case of the anisotropy $\Delta = 2$. Compared with Fig. 4(a), the output concurrence occurs in both the cases of coupling region ($J_2 < 0$ and $J_2 > 0$) in Fig. 4(b). In the case of the antiferromagnetic coupling region, for $\Delta = 2$ the critical temperature obviously increases (e.g., when $J_2 = -1$, $-2$, $-3$, and $-4$, the critical temperature $T_{\text{c}} = 0.86$, 1.74, 2.64, and 3.52, respectively.) This indicates that the anisotropy promotes the generation of the output concurrence again. From Fig. 4, it is observed that the output concurrence $C_{\text{out}}$ is dependent on the sign of $J_2$. The physical origin of the phenomenon can be explained as follows. As the mentioned above, the coupling parameter $J_2$ denotes the Heisenberg interaction between $Cu^{2+}$–$Mn^{2+}$ magnetic ions in the heterotrimetallic coordination compounds Fe–Mn–Cu. The coupling parameter $J_2 > 0$ corresponds to the ferromagnetic case, and $J_2 < 0$ to the

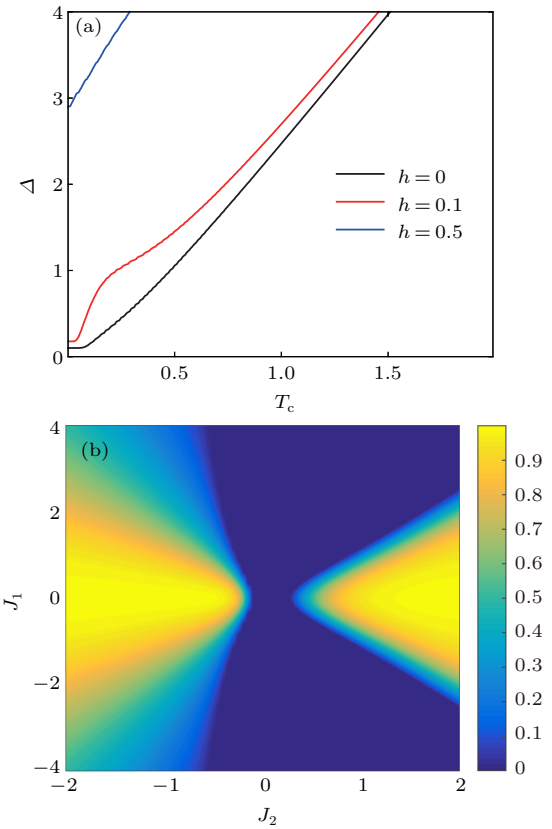



**Fig. 5.** (a) The dependence of the anisotropy parameter $\Delta$ on the critical temperature $T_{\text{c}}$ for different values of the external magnetic field $h$ with $J_1 = J_2 = -1$ and $C_{\text{in}} = 1$. (b) The density plot of the output concurrence depending on the Ising coupling parameter $J_1$ and the Heisenberg coupling parameter $J_2$ for $T = 0.1$, $\Delta = 2$, $h = 0$, and $C_{\text{in}} = 1$.

antiferromagnetic case. $\Delta$ is the anisotropy parameter. When $\Delta = 1$, the anisotropic model becomes the isotropic model. Through the straight calculating, it is found that in the isotropic case (i.e., $\Delta = 1$) for the antiferromagnetic case ($J_2 < 0$), the ground state of the Heisenberg interaction between $Cu^{2+}$-$Mn^{2+}$ magnetic ions is a maximally entangled state, while for the ferromagnetic case ($J_2 > 0$), the ground state corresponds to the nonentangled state. On the other hand, when $\Delta = 2$, for both the ferromagnetic case ($J_2 > 0$) and the antiferromagnetic case ($J_2 < 0$), the ground states are entangled, whereas the eigenvalues of the ground states in the two cases are different.

Now we study the effect of the external magnetic field on the output concurrence in Fig. 5(a). We plot the dependence of $\Delta$ on $T_c$ for $h = 0$, 0.1, and 0.5 with $J_1 = J_2 = -1$ and $C_{in} = 1$. The areas surrounded by the curve and the $y$-axis represent the occurrence of the entanglement. Obviously, as the magnitude of the external magnetic field increases, the area of the entanglement becomes smaller and smaller, and eventually disappears completely. This means that the external magnetic field will destroy the formation of the entanglement. Finally, we also study the density plot of $C_{out}$ depending on $J_1$ and $J_2$ for $T = 0.1$, $\Delta = 2$, $h = 0$ and $C_{in} = 1$ in Fig. 5(b). It is shown that the result of the output entanglement is symmetric with respect to $J_1 = 0$. In addition, the range of $C_{out}$ of $J_2 < 0$ is larger than that of $J_2 > 0$.

### 3.2. The average fidelity of entangled state teleportation

As we know, the average fidelity $F_A$ is to describe the quality of the process of teleportation. In order to transmit a quantum state better than the classical communication protocol, $F_A$ must be greater than $2/3$, which is the best fidelity in the classical word.[49] Now we will illustrate the behavior of the average fidelity in the standard teleportation protocol. In Fig. 6, we depict the average fidelity $F_A$ as functions of temperature $T$ and $\Delta$ for $J_1 = J_2 = -1$. The yellow region corresponds to the maximum average fidelity $F_A = 1$, and the blue region represents the minimum $F_A = 0$. The red curve surrounding the yellow region is the region where the quantum teleportation will become successful ($F_A > 2/3$), whereas the outside means that the quantum teleportation fails. We consider the case without the external magnetic field (i.e., $h = 0$) in Fig. 6(a), and the case with $h = 0.3$ in Fig. 6(b). It clearly shows that the region of successful fidelity with the case of $h = 0$ is greater than that of $h = 0.3$.

In Fig. 7, we discuss the effect of the Heisenberg coupling parameter $J_2$ on the average fidelity $F_A$ for $J_1 = -1$, $h = 0$ and various $T$. First, we consider the case with $\Delta = 1$ in Fig. 7(a). The dark, red, and blue curves correspond to the case with $T = 0.1$, 0.6, and 1, respectively. The dark dotted line denotes the best fidelity $2/3$ in the classical system. It is clearly shown that the teleportation will be successful only when $J_2 < 0$, and

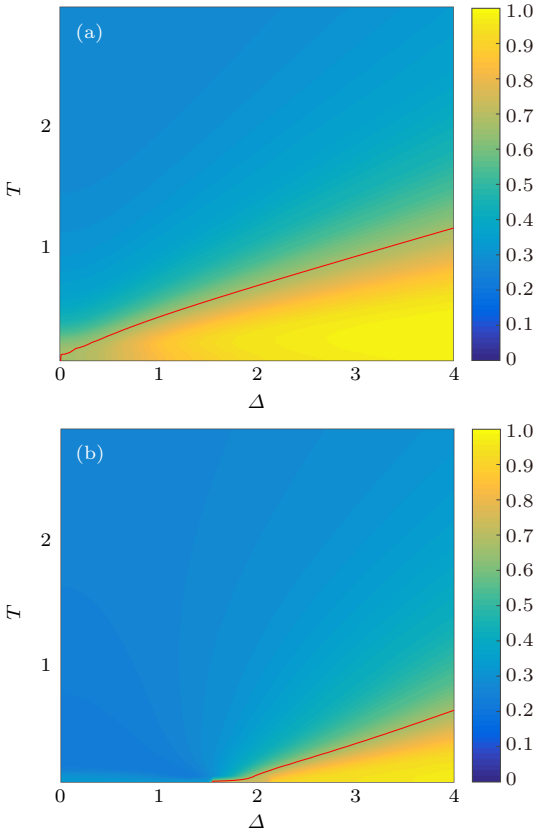



**Fig. 6.** The density plot of the average fidelity $F_A$ as functions of $T$ and $\Delta$ for $J_1 = J_2 = -1$: (a) $h = 0$, (b) $h = 0.3$. Here the red curve corresponds to $F_A = 2/3$.

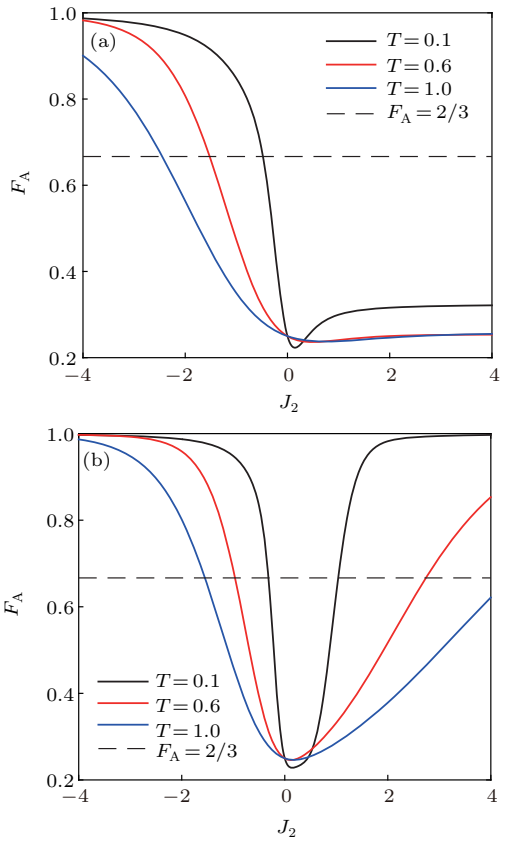



**Fig. 7.** The average fidelity $F_A$ as a function of $J_2$ for $J_1 = -1$, $h = 0$ and various $T$: (a) $\Delta = 1$, (b) $\Delta = 2$.

with increasing the temperature, it needs the larger antiferro-

magnetic coupling $J_2$ to ensure $F_A > 2/3$. Moreover, all the curves will eventually reach an uniform maximum as the antiferromagnetic coupling parameter increases. For example, when $T = 0.1$, $J_2 \leq -0.48$, the average fidelity $F_A$ will be larger than $2/3$, and finally up to $F_A \approx 1$. The change trends of curves of $T = 0.6$ and 1 are similar to those with $T = 0.1$. We also study the case of the anisotropy ($\Delta = 2$) in Fig. 7(b). Compared with Fig. 7(a), it is obvious that there exists the successful average fidelity when $J_2 > 0$ in Fig. 7(b).

Finally, we investigate the effect of the external magnetic field $h$ on the average fidelity, and plot $F_A$ as a function of $h$ for different $T$ in Fig. 8. We observe the case with $\Delta = 1$ in Fig. 8(a). It is shown that when the magnitude of the external magnetic field increases, the average fidelity decreases sharply firstly, then gets the minimum. After that, it gradually increases and finally stabilizes at $F_A = 0.333$. Taking $T = 0.6$ for instance, when $h = 0$, the average fidelity $F_A = 0.8074$. When $h = 0.75$, the average fidelity gets the minimum 0.2268. Lastly when $h = 2.52$, the average fidelity gets the stable value 0.333. In addition, the average fidelity is always smaller than $2/3$ with increasing the temperature (e.g., $T = 1$). The case of $\Delta = 2$ is plotted in Fig. 8(b). It is shown that the increasing magnitude of the anisotropy will suppress the effect of the temperature on the average fidelity for a weak external magnetic field. However, when the external magnetic field is enough high, the average fidelity always keeps 0.333, that is, in this case the quantum teleportation fails.

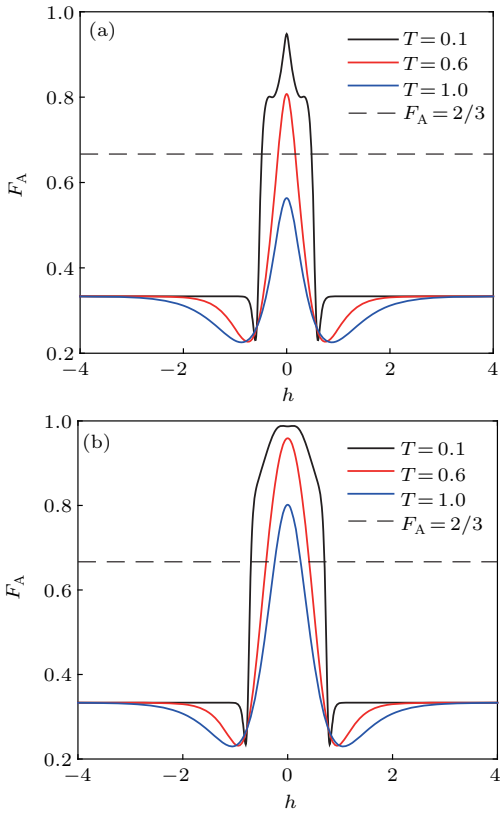



**Fig. 8.** The average fidelity $F_A$ as a function of $h$ for $J_1 = -1$ and $J_2 = -2$ at various $T$: (a) $\Delta = 1$, (b) $\Delta = 2$.

## 4. Conclusions

We have studied the quantum teleportation of a spin-1/2 Ising–Heisenberg chain, which can describe some features of the heterotrimetallic Fe–Mn–Cu coordination polymer. The teleported state we consider here is an arbitrary entangled state, and we have obtained analytical results for the input concurrence, the output concurrence and the average fidelity. The results show that the output concurrence can be enhanced by the input state concurrence $C_{in}$, the anisotropy coupling $\Delta$ and the Heisenberg coupling $J_2$. In addition, a certain temperature $T$ can also promote entanglement when the anisotropy parameter is small. However, the external magnetic field and high temperature will inhibit the generation of the entanglement. The average fidelity $F_A$ of the entangled state teleportation as a function of the temperature $T$, the anisotropy $\Delta$, the Heisenberg coupling $J_2$ and the external magnetic field $h$ are discussed in detail. It is shown that the anisotropy $\Delta$ and the Heisenberg coupling $J_2$ not only promote the generation of the entanglement but also expand the scope of the successful average fidelity.

## References


[1] Nielson M A and Chuang I L 2000 *Quantum computation and quantum information* (Cambridge: Cambridge University Press)
[2] Bennett C H, Brassard G, Crépeau C, Jozsa R, Peres A and Wootters W K 1993 *Phys. Rev. Lett.* **70** 1895
[3] Bouwmeester D, Pan J W, Mattle K, Eibl M, Weinfurter H and Zeilinger A 1997 *Nature* **390** 575
[4] Ekert A K 1991 *Phys. Rev. Lett.* **67** 661
[5] Deng F G and Long G L 2003 *Phys. Rev. A* **68** 042315
[6] Hillery M, Bužek V and Berthiaume A 1999 *Phys. Rev. A* **59** 1829
[7] Cleve R, Gottesman D and Lo H K 1999 *Phys. Rev. Lett.* **83** 648
[8] Bennett C H and Wiesner S J 1992 *Phys. Rev. Lett.* **69** 2881
[9] Popescu S 1994 *Phys. Rev. Lett.* **72** 797
[10] Bowen G and Bose S 2001 *Phys. Rev. Lett.* **87** 267901
[11] Boschi D, Branca S, de Martini F, Hardy L and Popescu S 1998 *Phys. Rev. Lett.* **80** 1121
[12] Furusawa A, Sørensen J L, Braunstein S L, Fuchs C A, Kimble H J and Polzik E S 1998 *Science* **282** 706
[13] Yin J, Ren J G, Lu H, Cao Y, Yong H L, Wu Y P, Liu C, Liao S K, Zhou F, Jiang Y, Cai X D, Xu P, Pan G S, Jia J J, Huang Y M, Yin H, Wang J Y, Chen Y A, Peng C Z and Pan J W 2012 *Nature* **488** 185
[14] Ma X S, Herbst T, Scheidl T, Wang D, Kropatschek S, Naylor W, Wittmann B, Mech A, Kofler J, Anisimova E, Makarov V, Jennewein T, Ursin R and Zeilinger A 2012 *Nature* **489** 269
[15] Ren J G, Xu P, Yong H L, Zhang L, Liao S K, Yin J, Liu W Y, Cai W Q, Yang M, Li L, Yang K X, Han X, Yao Y Q, Li J, Wu H Y, Wan S, Liu L, Liu D Q, Kuang Y W, He Z P, Shang P, Guo C, Zheng R H, Tian K, Zhu Z C, Liu N L, Lu C Y, Shu R, Chen Y A, Peng C Z, Wang J Y and Pan J W 2017 *Nature* **549** 70
[16] Stenholm S and Bardroff P J 1998 *Phys. Rev. A* **58** 4373
[17] Braunstein S L and Kimble H J 1998 *Phys. Rev. Lett.* **80** 869
[18] Vaidman L 1994 *Phys. Rev. A* **49** 1473
[19] Lee J and Kim M S 2000 *Phys. Rev. Lett.* **84** 4236
[20] Arnesen M C, Bose S and Vedral V 2001 *Phys. Rev. Lett.* **87** 017901
[21] Wang X 2001 *Phys. Rev. A* **64** 012313
[22] Kamta G L and Starace A F 2002 *Phys. Rev. Lett.* **88** 107901
[23] Zhou L, Song H S, Guo Y Q and Li C 2003 *Phys. Rev. A* **68** 024301
[24] Zhang G F and Li S S 2005 *Phys. Rev. A* **72** 034302
[25] Yeo Y 2002 *Phys. Rev. A* **66** 062312
[26] Yeo Y, Liu T, Lu Y E and Yang Q Z 2005 *J. Phys. A* **38** 3235
[27] Zhang G F 2007 *Phys. Rev. A* **75** 034304
[28] Hao X and Zhu S 2005 *Phys. Lett. A* **338** 175
[29] Guo J L, Xia Y and Song H S 2008 *Opt. Commun.* **281** 2326

[30] Cai J T, Abliz A, Zhang G F and Bai Y K 2010 *Opt. Commun.* **283** 4415
[31] Qin W and Guo J L 2015 *Int. J. Theor. Phys.* **54** 2386
[32] Xi Y X, Cheng W W and Huang Y X 2015 *Quantum Inf. Process.* **14** 2551
[33] Rojas M, de Souza S M and Rojas O 2017 *Ann. Phys.* **377** 506
[34] Kikuchi H, Fujii Y, Chiba M, Mitsudo S and Idehara T 2003 *Physica B* **329–333** 967
[35] Ishikawa R, Katoh K, Breedlove B K and Yamashita M 2012 *Inorg. Chem.* **51** 9123
[36] Zhang W X, Ishikawa R, Breedlove B and Yamashita M 2013 *Rsc Adv.* **3** 3772
[37] Wang Z X, Zhang X, Zhang Y Z, Li M X, Zhao H, Andruh M and Dunbar K R 2014 *Angew. Chem. Int. Ed.* **53** 11567
[38] Leuenberger M N and Loss D 2001 *Nature* **410** 789
[39] Ardavan A, Rival O, Morton J J L, Blundell S J, Tyryshkin A M, Timco G A and Winpenny R E P 2007 *Phys. Rev. Lett.* **98** 057201
[40] Rojas O, Rojas M, Ananikian N S and de Souza S M 2012 *Phys. Rev. A* **86** 042330
[41] Rojas O, Rojas M, de Souza S M, Torrico J, Strečka J and Lyra M L 2017 *Physica A* **486** 367
[42] Zheng Y, Mao Z and Zhou B 2018 *Chin. Phys. B* **27** 090306
[43] Qiao J and Zhou B 2015 *Chin. Phys. B* **24** 110306
[44] Wang H, Zhang L F, Ni Z H, Zhong W F, Tian L J and Jiang J 2010 *Cryst. Growth* **10** 4231
[45] Souza F, Lyra M L, Strečka J and Pereira M S S 2019 *J. Magnet. Magnet. Mater.* **471** 423
[46] Wootters W K 1998 *Phys. Rev. Lett.* **80** 2245
[47] Hill S and Wootters W K 1997 *Phys. Rev. Lett.* **78** 5022
[48] Jozsa R 1994 *J. Mod. Opt.* **41** 2315
[49] Bowdrey M D, Oi D K L, Short A J, Banaszek K and Jones J A 2002 *Phys. Lett. A* **294** 258